Global Biogeochemical Cycles

Supporting Information for

Oxygen saturation surrounding deep-water formation events in the Labrador Sea from Argo-O₂ data

Mitchell K. Wolf[1], Roberta C. Hamme[1], Denis Gilbert[2], Igor Yashayaev[3], and Virginie Thierry[4]

[1]School of Earth and Ocean Sciences, University of Victoria, P.O. Box 1700 STN CSC, Victoria, BC, Canada V8W 2Y2,
[2]Maurice-Lamontagne Institute, Fisheries and Oceans Canada, Mont-Joli, Quebec, Canada G5H 3Z4,
[3]Bedford Institute of Oceanography, Fisheries and Oceans Canada, Dartmouth, Nova Scotia, Canada B2Y 4A2,
[4]Ifremer, Laboratoire d'Océanographie Physique et Spatiale, UMR 6523 CNRS-IFREMER-IRD-UBO, Plouzané, France.

Contents of this file

Figures S1 to S5
Table S1

Introduction

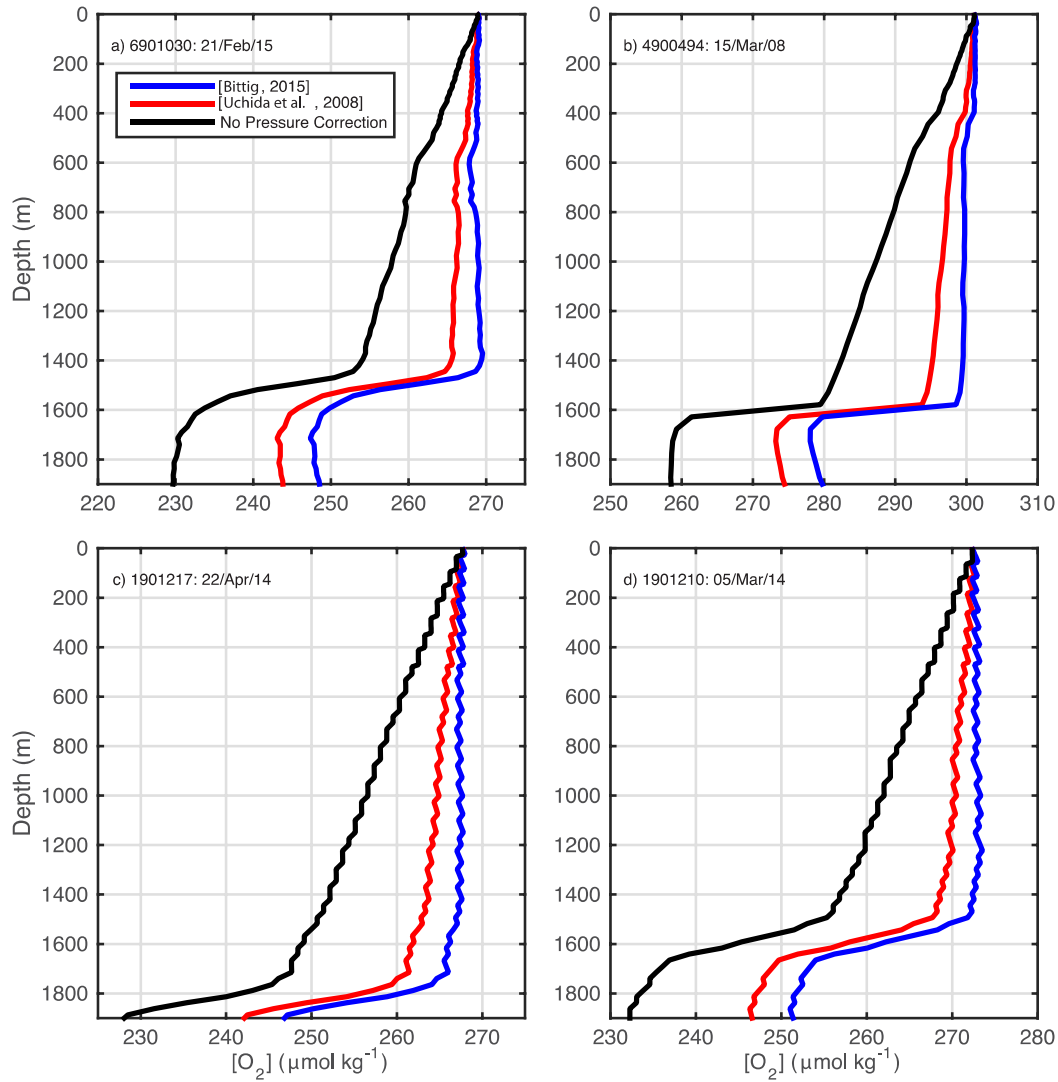This supplementary information file provides additional or more complete figures and tables.

Figure S1. Oxygen concentration profiles during deep convection with various pressure corrections applied from four floats (float number and profile date indicated in top left corners). Pressure corrections shown are based on *Bittig et al.* [2015] (blue line), or *Uchida et al.*, [2008] (red line), with data having no pressure correction shown as well (black line).
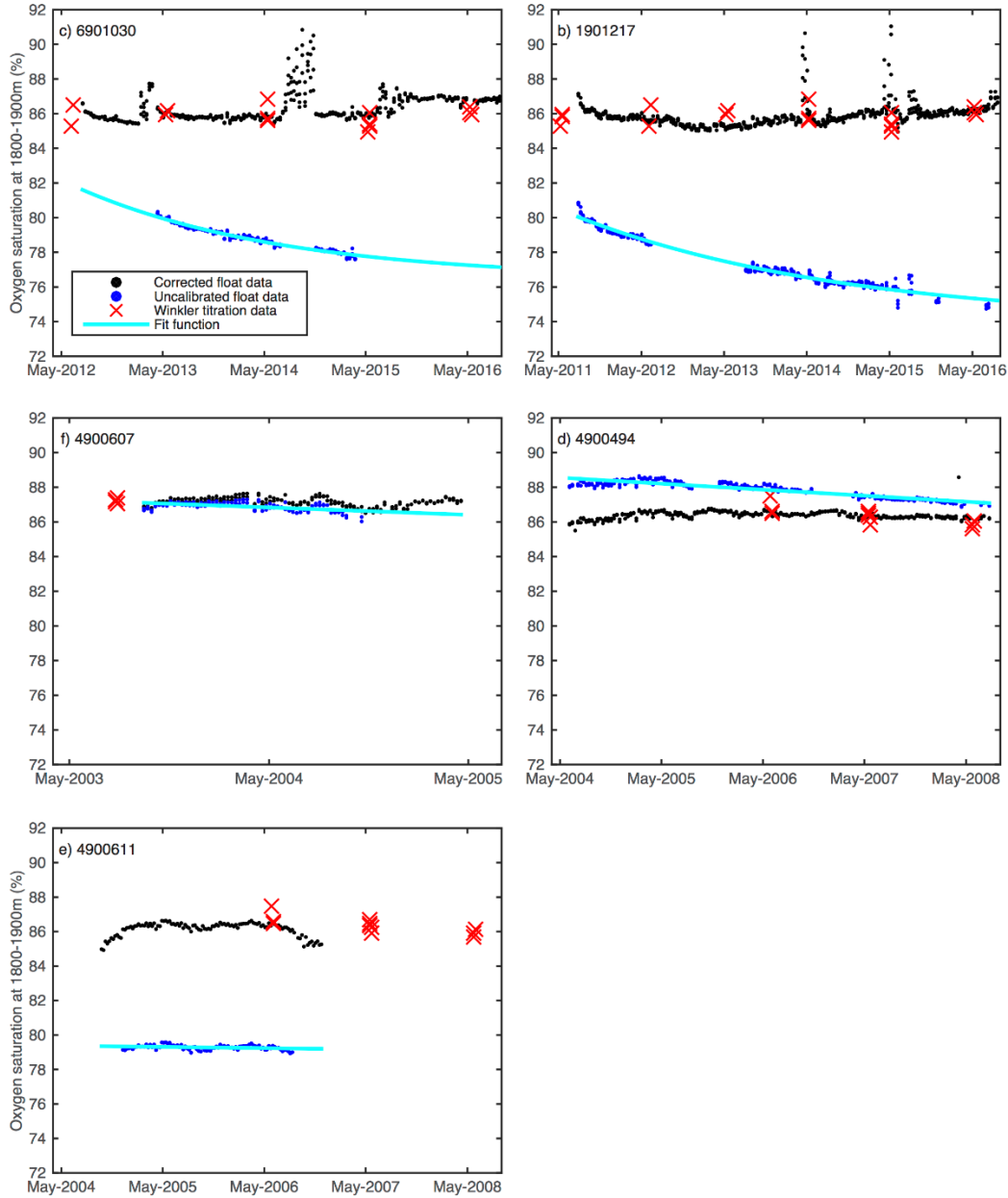
Figure S2. Corrected float-measured oxygen saturation (%) between the depths 1800m to 1900m (black dots) compared to the uncalibrated float data for the same depths used for the fit calculation (blue dots) for five floats (float number indicated in top left corners). The exponentially decaying fit function (light blue line in a, b, and c) is calculated from Equation 2 while the linearly decaying fit function (light blue line in d, e, and f) is calculated from Equation 3. Winkler titration data at these depths from annual May surveys of the AR7W hydrographic line is shown in red crosses. Similar figure for float 1901210 is shown in Figure 2.
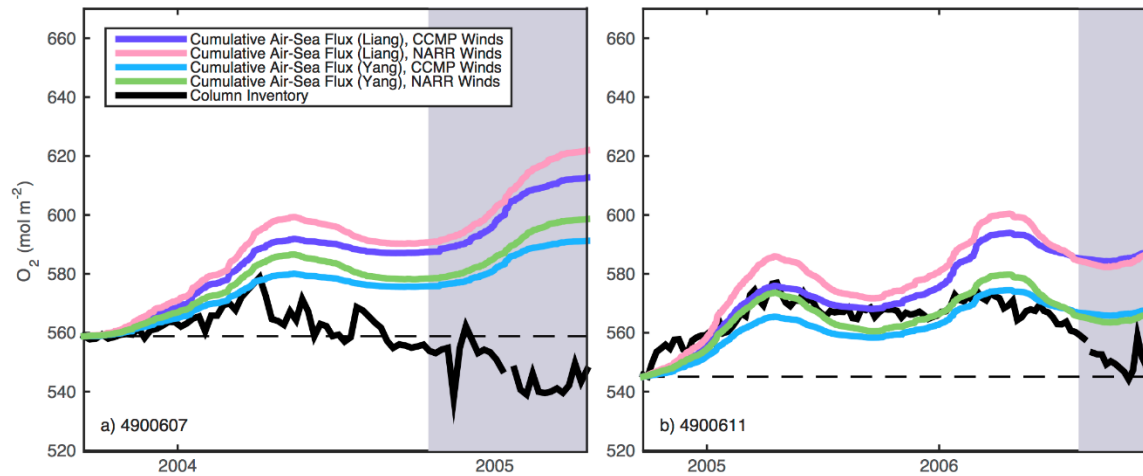
Figure S3. Time series of the cumulative air-sea flux (mol m^{-2}) calculated using the *Liang et al.* [2013] gas exchange parameterization with CCMP winds (purple line) and NARR winds (pink line), and the *Yang et al.* [2017] parameterization with CCMP winds (blue line) and NARR winds (green line) compared to the oxygen column inventory from 0 to 1900 m (solid black line) for two floats (float number indicated in lower left corners). The grey shaded regions represent time periods when the float left the study region (Figure 1).
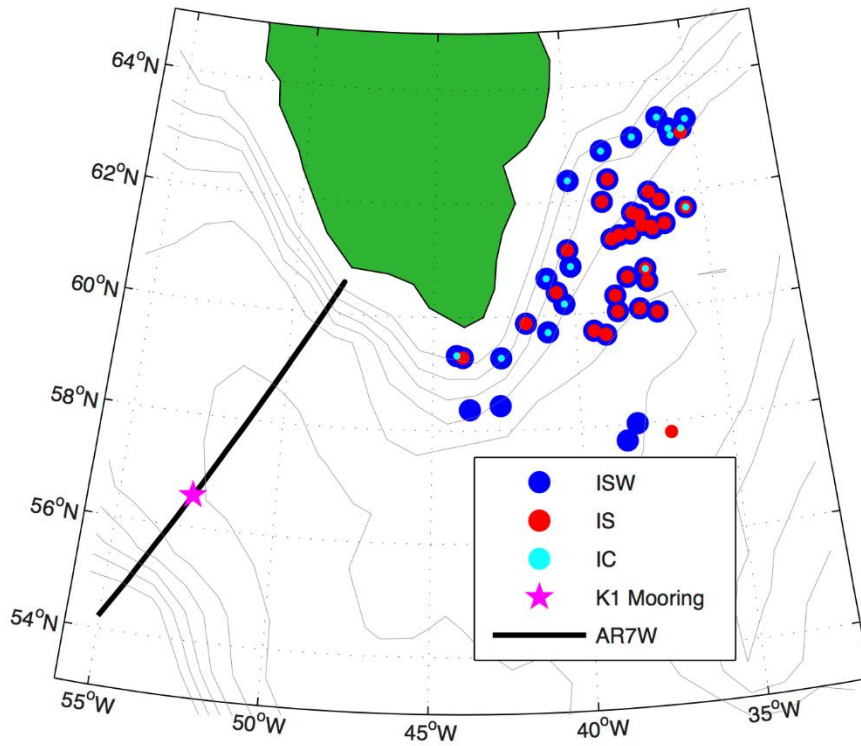
Figure S4. Map of profile locations in the Irminger Sea from floats 1901210 and 6901030. The size of the dot represents the average depth of the water mass, with Icelandic Slope Water (ISW, blue circles) at 1270 ± 83 m, Irminger Sea water (IS, red circles) at 742 ± 28 m, and Irminger Current water (IC, cyan circles) at 290 ± 58 m. Also shown is the location of the K1 mooring site (pink star) and the AR7W hydrographic line by Fisheries and Oceans Canada (black line). Grey lines indicate bathymetry at 500 m intervals, starting at 1000 m.
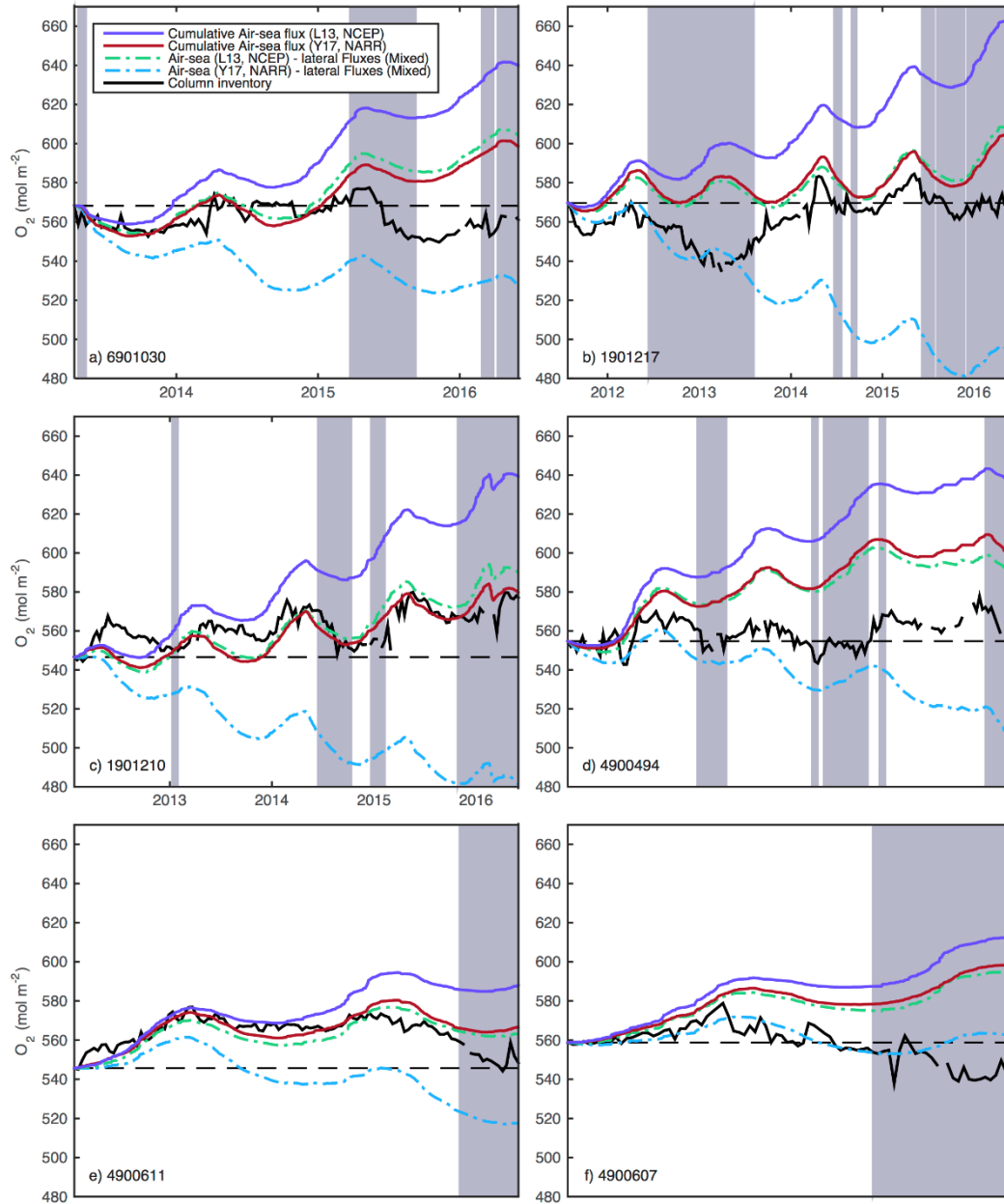
Figure S5. Time series of the cumulative air-sea flux (mol m^{-2}) calculated using the *Liang et al.* [2013] (L13) gas exchange parameterization with NCEP winds (solid purple line) and the *Yang et al.* [2017] (Y17) parameterization with NARR winds (solid dark red line) compared to the oxygen column inventory from 0 to 1900 m (solid black line) for all six floats (float number indicated in lower left corners). The cumulative combination of the lateral flux from the mixed choice for the warmer water mass (25% IS, 25% IC 50% ISW) and the air-sea fluxes are also shown: *Liang et al.* [2013] (L13) with NCEP winds (dashed green line) and *Liang et al.* [2017] (Y17) with NARR winds (dashed blue line). The grey shaded regions represent time periods when the float left the study region (Figure 1).

6

Table S1. Annual Average Air-Sea Oxygen Flux (mol m^{-2} yr^{-1}) and Inventory Gain

Float ID	Flux[a] (Liang[b], CCMP[c])	Flux[a] (Liang[b], NARR[d])	Flux[a] (Yang[e], CCMP[c])	Flux[a] (Yang[e], NARR[d])	Inventory Gain[f]
Float 1901210 Corrected[g] O$_2$	21.36	17.43	10.74	7.64	6.38
Float 1901210 Uncorrected[h] O$_2$	83.71 (40.70)	108.89 (45.67)	57.34 (25.12)	79.67 (29.77)	0.71 (0.75)
Float 1901217 Corrected[g] O$_2$	18.82	16.29	9.28	6.61	-1.74
Float 1901217 Uncorrected[h] O$_2$	94.63 (46.60)	134.44 (59.22)	66.74 (30.28)	100.06 (40.52)	-8.11 (-8.70)
Float 6901030 Corrected[g] O$_2$	22.91	19.21	12.40	9.72	-4.55
Float 6901030 Uncorrected[h] O$_2$	86.90 (39.42)	112.29 (42.84)	60.82 (24.84)	83.88 (28.49)	-10.20 (-10.93)
Float 4900494 Corrected[g] O$_2$	19.97	19.07	11.26	10.59	2.77
Float 4900494 Uncorrected[h] O$_2$	10.01 (24.72)	4.40 (26.49)	3.72 (14.96)	-1.08 (16.63)	0.59 (0.57)
Float 4900607 Corrected[g] O$_2$	33.87	39.71	20.38	25.03	-7.10
Float 4900607 Uncorrected[h] O$_2$	38.19 (37.09)	46.30 (44.64)	23.59 (22.77)	30.15 (28.86)	-9.77 (-9.78)
Float 4900611 Corrected[g] O$_2$	19.59	19.17	10.48	9.70	1.27
Float 4900611 Uncorrected[h] O$_2$	76.00 (20.08)	105.07 (19.93)	53.74 (10.86)	78.55 (10.31)	0.72 (0.79)

[a] Average annual air-sea oxygen flux over entire float lifetime

[b] *Liang et al.* [2013]

[c] Cross-calibrated multi-platform (CCMPv2) surface vector winds [*Atlas et al.*, 2011; *Wentz et al.*, 2015]

[d] North American Regional Reanalysis (NARR) surface vector winds [*Mesinger et al.*, 2006]

[e] *Yang et al.* [2017]

[f] Total inventory gain from 0-1900m over entire float lifetime

[g] Oxygen dataset calibrated following Section 3

[h] Uncalibrated oxygen dataset, with values from only storage drift correction (not in-situ drift) in brackets